

DEVELOPMENT AND CHARACTERIZATION OF UNMODIFIED KAOLINITE / EVOH NANOCOMPOSITES BY MELT COMPOUNDING

Luis Cabedo^{1*}, María Pilar Villanueva¹, José María Lagarón², Enrique Giménez³

¹Polymers and Advanced Materials Group (PIMA), Universidad Jaume I, 12071, Castellón, Spain.

³Novel Materials and Nanotechnology, IATA-CSIC, Aptdo. Correos 73, 46100 Burjassot, Spain

³Instituto de Tecnología de Materiales, Universidad Politécnica de Valencia (UPV), Camino de Vera s/n,
46022 Valencia (SPAIN)

(Corresponding author e-mail: lcabedo@uji.es)

Abstract

Nanocomposites of unmodified kaolinite (Kaol) / ethylene-vinyl alcohol copolymer (EVOH) with different Kaol contents have been obtained by a two-step process: melt blending in an internal mixer and film processing by co-extruding the obtained clay polymer nanocomposites pellets in between two low-density polyethylene (LDPE) layers. The addition of the clay mineral to the molten polymer has been carried out by using a Kaol/EVOH masterbatch containing 15mass% Kaol. The so-obtained samples have been analysed by means of WAXS, SEM, TEM, DMA and tensile tests. Finally, barrier properties to water vapour and oxygen at two relative humidities have been assessed. Morphological analysis has revealed high degree of dispersion and distribution of the Kaol within the EVOH matrix. A considerable increase in the mechanical and in the barrier properties has been found. The present work puts forward the effectiveness of an unmodified kaolinite for obtaining ultra-high barrier clay mineral / polymer nanocomposites.

1. Introduction

Ethylene-vinyl alcohol (EVOH) copolymers are a family of semi-crystalline random copolymers widely used in the food-packaging sector due to their outstanding gas barrier properties to oxygen and organic compounds (solvents and food aromas); as well as their considerable chemical resistance and high transparency(Lagaron et al., 2001). The major drawback of these materials is their moisture sensitivity that causes a significant decrease in their gas barrier properties at high relative humidities(Lagarón et al., 2001; Muramatsu et al., 2003; Cava et al., 2006; Kim et al., 2014). Therefore, EVOH is commonly used as a barrier intermediate layer in co-extruded multilayer structures, being hence protected by layers of hydrophobic materials such as polyolefins(Villalpando-Olmos et al., 1999). The presence of EVOH in the packaging structure is key to food quality and safety, because it reduces the ingress of oxygen and the loss of aroma components during extended packaging shelf-life(Martínez-Sanz et al., 2012).

It is well known that the addition of nanofillers to a pure polymer can lead to an increase in some relevant material properties, such as mechanical properties or thermal stability, without significant reductions in toughness and transparency(Alexandre and Dubois, 2000; Kotsilkova et al., 2001; Sinha Ray and Okamoto, 2003; Wan et al., 2003; Pavlidou and Papaspyrides, 2008). In the particular case of the EVOH copolymers, it has been widely reported that the addition of clay-based nanofillers is a convenient approach to increase the barrier properties mainly due to an increase in the tortuosity of the diffusion path(Gimenez et al., 2004; Lagarón et al., 2005; Arora and Padua, 2010; Ophir et al., 2010; Kim et al., 2014; Kim and Cha, 2014).

Among the clay polymer nanocomposites (CPN) the most widely studied clay mineral is montmorillonite (Mt) due to its large cation exchange capacity which facilitates the organomodification enhancing its dispersion in polymer matrices(Giannelis, 1996; Lambert and Bergaya, 2013). However, the kaolinite (Kaol) has been also a very suitable clay mineral for obtaining CPN (Chen and Evans, 2005; Arora and Padua, 2010; Vahabi et al., 2012; Detellier and Letaief, 2013; Zulfiqar et al., 2015), despite the problem associated to its chemical structure which makes it difficult to organomodify permanently (Kenne and Detellier, 2016) . In previous works, Kaol CPN with different polymer matrix have been successfully obtained(Cabedo et al., 2004, 2006b, 2009; Villanueva et al., 2010; Fukushima et al., 2012). For the particular case of EVOH / Kaol

CPN a decrease in oxygen permeability at 45°C from $3.6 \cdot 10^{-5} \text{ (cm}^3 \text{ m)/ (m}^2 \text{ day atm)}$ to less than $10^{-5} \text{ (cm}^3 \text{ m)/ (m}^2 \text{ day atm)}$ was achieved (Cabedo et al., 2004).

Kaol is a very common material in earth and is widely used as raw material in several industrial sectors. Kaolinite ($\text{Al}_2\text{Si}_2\text{O}_5(\text{OH})_4$) is a 1:1 clay mineral that is composed of silicon oxide tetrahedral sheets bonded to aluminium oxide/hydroxide (gibbsite) octahedral sheet (Schoonheydt and Johnston, 2006). This particular structure leads to an asymmetric configuration that is responsible for the formation of hydrogen bonds between consecutive layers, thus leading to a large cohesive energy. As a consequence of these strong layer-to-layer interactions, intercalation of polymeric chains between the Kaol layers is not favoured. For this reason, it is necessary a previous chemical treatment to facilitate the intercalation and potential exfoliation of Kaol during the melt mixing (Yoshihiko et al., 1999; Gardolinski et al., 2000; Kenne and Detellier, 2016; Zhang et al., 2016). The chemical modification of the clay mineral surface, necessary for achieving a good degree of dispersion of the Kaol, can interact negatively with the polymer (Fornes et al., 2003; Bordes et al., 2009) or even migrate to the food (Xia et al., 2015). These are potential drawbacks for the use of Kaol in food packaging applications. In this work, however, a different approach is explored: an EVOH/Kaol masterbatch. This approach is very convenient since the clay mineral is incorporated to the polymer in a highly dispersed condition, hence being the shear forces applied during compounding enough to obtain a favourable morphology in a non-modified Kaol. Moreover, the masterbatch route can be implemented in conventional polymer compounding equipment in normal operating conditions without significant modification of the process.

This work aims at exploring the masterbatch route for obtaining unmodified Kaol / EVOH nanocomposites with improved performance for food packaging applications. The morphological characteristics, mechanical properties and oxygen and water barrier properties of the materials developed are also reported as a function of the Kaol content.

2. Experimental

2.1. Materials

The ethylene-vinyl alcohol copolymer (EVOH) used in this work was a commercial grade (Soarnol®), containing 32mol% ethylene, kindly supplied by The Nippon Synthetic Chemical Industry Co., Ltd. (NIPPON GOHSEI).

The clay mineral was a natural kaolinite supplied by Arciblansa (Alcora, Spain). The isopropanol (>99.7%) was purchased from Sigma Aldrich and used as received.

2.2. Masterbatch preparation

Unmodified Kaol/EVOH masterbatch was prepared according to Cabedo(Cabedo, 2007). For so, EVOH pellets were dissolved in an isopropanol / water solution (50 / 50 by volume) at 90°C under constant stirring. A Kaol dispersion was prepared in the same solvent composition at similar conditions. Once the polymer was fully dissolved the Kaol dispersion was added dropwise to the polymer solution and kept for 12 hour at 90°C and constant stirring. The system is then precipitated by pouring it into a container of cold water, milled and dried under vacuum. The masterbatch composition was 15weight% of Kaol.

2.3. CPN processing

The CPN were processed by melt blending in an internal mixer (Rheomix-Haake) during a mixing time of 5 minutes at a temperature of 210°C and rotor speed of 40 rpm. Prior to the blending step, both masterbatch and polymer were dehumidified at 100°C during an hour in a Piovani. The masterbatch was added to the mixer once the polymer was fully melted. The CPN resulting of the mixing was cooled with liquid nitrogen and grinded into powder in a rotating mill. CPN with three different Kaol contents were obtained: 2.5, 5 and 7weight% (further referred as EVOH/2.5Kaol, EVOH/5Kaol and EVOH/7Kaol respectively).

The CPN powder was transformed into samples with two different thicknesses: plates (0.8mm) and films (15µm). The plates were obtained by compression moulding at 200°C and 4 manometric bars during 2 minutes and allowed to cool to room temperature

under pressure at a cooling rate of 20°C/min. The so-obtained plates were used for the morphological and DMA characterization. 20µm thick films of the 2.5% and 5% Kaol content samples were obtained by co-extrusion in between two 80µm thick layers of low-density polyethylene (LDPE) under identical conditions of a previous work(Cabedo, 2007). The co-extruded films were subsequently delaminated and the CPN layer used for the mechanical and barrier characterization.

2.3. Characterization techniques

WAXS (Wide Angle X-Ray Scattering) experiments were performed using a Bruker AXS D4 Endeavour instrument (Bruker Corporation, Karlsruhe, Germany) equipped with an automatic sample change system. Radial scans of intensity versus scattering angle (2θ) were recorded at room temperature in the range 2° to 30° (2θ). The step size was 0.02° (2θ) and the scanning rate was 8s/step. The X-ray source used was a filtered Cu K $_{\alpha}$ radiation tube ($\lambda = 1.54\text{\AA}$), at an operating voltage of 40kV and a filament current of 40mA. The sample holder allows rotating the sample in-plane, removing thus any in-plane orientation effect. Bragg's law was applied to calculate clay mineral basal spacing.

The scanning electron microscopy (SEM) experiments were developed using a LEO 440i (Leo Electron Microscopy, Cambridge, UK) equipped with a digital image acquisition system. Normal operating conditions were 20kV and 100pA for the secondary electron detector. The polymeric samples were cryofractured in liquid nitrogen and coated by sputtering with Au-Pd.

Transmission electron microscopy (TEM) was performed using a JEOL 1010 (Jeol Ltd, Akishima, Japan) equipped with a digital Bioscan (Gatan) image acquisition system. TEM observations were performed on ultra-thin sections of cryoultramicrotomed CPN sheets.

Dynamic-mechanical experiments were performed in a Perkin Elmer DMA 7e (Perkin Elmer, Waltham, USA) equipment in three-point bending mode. The temperature range registered was from -90°C to 150°C at a heating rate of 5°C/min, at 1Hz frequency and a

dynamic deformation of 0.15%.

Tensile testing up to failure was carried out at room temperature on an Instron 4469 H1907 Universal Tester (Instron Norwood, USA). A fixed crosshead rate of 10 mm/min was utilized in all cases and the results were taken as the average of five tests. Dumb-bell shaped specimens according to ASTM D638 were used. Experiments of the co-extruded films were conducted both in the machine direction (MD) and in the transverse direction (TD).

The oxygen transmission rate through vacuum dried co-extruded film specimens was measured at room temperature under two relative humidity conditions (0% R.H. and 80% R.H.) using an Oxtran 2/21 (Modern Control Inc., MN, USA, MOCON) instrument. The carrier gas was nitrogen while the ambient gas was oxygen with 99.9% purity. The surface analysed was in all cases 50 cm².

Direct permeability to water vapour was measured from the slope of the weight loss–time curves at 24°C and 40% RH. The films were sandwiched between the aluminium top (open O-ring) and bottom (deposit for the permeant) parts of a specifically designed permeability cell with screws. A Viton rubber O-ring was placed between the film and the bottom part of the cell to enhance sealability. Then the bottom part of the cell was filled with water and the pinhole secured with a rubber O-ring and a screw. Finally, the cell was placed in an environment with controlled moisture of 40% RH and the water weight loss through a film area of 0.001 m² was monitored and plotted as a function of time. Cells with aluminium films (with a thickness of ca. 10 µm) were used as control samples to estimate water loss through the sealing. The permeability sensibility of the permeation cells was determined to be better than 0.01 · 10⁻¹³ kg · m/s · m² · Pa based on the weight loss measurements of the aluminium cells. Cells clamping polymer films but with no solvent were used as blank samples to monitor water uptake. Water vapour permeation rates were estimated from the steady-state permeation slopes. The tests were done in triplicate and average values and standard errors are provided.

3. Results and discussion.

3.1. Morphological analysis of kaolinite and kaolinite / EVOH nanocomposites.

SEM micrograph of the natural Kaol in its natural state is presented in Figure 1a. Imperfect stacking of the clay mineral platelets is detected, thus being the predominant microstructure a fine distribution of small sized Kaol aggregates with broken platelets and an uneven size distribution. WAXS pattern of the unmodified Kaol is plotted in Figure 1b. Since it is a natural clay without any kind of purification, other minor phases can be detected together with the Kaol; among them the more relevant are quartz and illite.

WAXS patterns of the powder masterbatch and the three CPN samples obtained by compression moulding direct from the CPN powder are presented in Figure 2. A reflection at $12.4^{\circ}(2\theta)$ in all patterns that can be associated to the basal reflection (001) of the Kaol, having thus a basal spacing of 0.72nm. This peak is visible in masterbatch and all CPN patterns, revealing the presence of Kaol in an aggregate state. Nevertheless, the low relative intensity of the basal reflection together with its high degree of imperfection would indicate either bad stacking of the clay or small size of the aggregates, or both. This is particularly noticeable for the masterbatch sample, although the Kaol content is much higher. Comparing the three CPN patterns, the intensity of the basal reflection of the clay mineral is higher in the EVOH/7Kaol diffractogram than in the lower content samples. This may indicate higher degree of aggregation in the former with respect to the other two, in which this reflection shows almost the same intensity, despite the difference in composition. Attending to this behaviour, it can be inferred that better morphology has been achieved in the EVOH/2.5Kaol and EVOH/5Kaol samples when compared to the EVOH/7Kaol sample. However, microscopy analysis is required to figure out the actual state of dispersion of the Kaol within the polymer matrix in these samples.

The reflection labelled EVOH in Figure 2 is ascribed in the scientific literature(Cerrada et al., 1998; J. M. Lagarón et al., 2001) to the (100) reflection of the ethylene-vinyl copolymer. In the pattern of the masterbatch this reflection is barely visible, which together with the low perfection of the other reflections associated to the EVOH, could be interpreted as a low crystallinity or a highly imperfect degree of cristallinity. On the other hand, the reflection appearing at $8.6^{\circ}(2\theta)$ corresponds to the (002) plane of an

illite, which is a very common natural impurity of kaolinitic clays. This impurity, having also a laminar structure, seems to collapse to its natural position during the CPN processing, since it is visible in all three CPN and not in masterbatch pattern.

SEM micrograph of the masterbatch powder at 5000X is shown in Figure 3. It is possible to detect the presence of small aggregates well integrated within the EVOH matrix. This reveals a good interaction between the unmodified Kaol surface and the polymer. SEM micrographs of the fractured surface of the EVOH/5Kaol and EVOH/7Kaol samples are presented in Figure 4. At a first glance, no major aggregates can be noticed, therefore, it can be said that in both cases the morphology of the CPN is highly favourable, i.e. high degree of dispersion of the Kaol platelets within the EVOH matrix. However, the presence of small aggregates (pointed in the micrograph with white arrows) can be noticed, which, in all cases, have a considerably high aspect ratio (length/thickness) and its thickness is in the nanometre range. The presence of these nanometric aggregates is higher in the sample containing 7% Kaol loading. This trend is also observed by means of TEM analysis (see Figure 5). In both cases, the Kaol is homogeneously dispersed throughout the analysed surface, revealing a high level of interaction between the clay mineral surface and the polymer matrix. The presence of nanometric aggregates can be detected in both samples, although is considerably higher in the EVOH/7Kaol, according to SEM results. These small sized aggregates, particularly in the EVOH/5Kaol, are small aggregated structures containing a low number of clay platelets stacked to each other at the natural distance. However, since the aspect ratio of these entities is very high and the thickness is below 100nm, the effect may not affect negatively to the final properties of the CPN.

Morphological analysis indicates that clay loadings beyond 5% lead to the aggregation of the Kaol under these particular processing conditions, therefore it can be inferred that the limit in the amount of Kaol that EVOH matrix can hold without collapsing is, in this system, around 5weight%. Small Kaol aggregates are detected in all the samples studied by means of WAXS and microscopic techniques, revealing the presence of a fraction of the clay mineral that cannot be fully exfoliated; however, attending to the high degree of delamination and the nanometer size of the residual Kaol aggregates, it can be said that favourable morphology is achieved, particularly in the EVOH/2.5Kaol and EVOH/5Kaol samples.

3.2. Mechanical and dynamic-mechanical properties of Kaolinite / EVOH nanocomposites.

DMA curves of the pure EVOH and the Kaol/EVOH nanocomposites are plotted in Figure 6. EVOH copolymers present three different relaxations in the temperature range analysed: the most relevant (α -relaxation) is ascribed to the mechanical relaxation due to the glass transition. The α' -relaxation is generally attributed to chain movement in the crystal boundaries and imperfect crystals and the β -relaxation is assigned to collaborative chain movements in shorter fragments than the α -relaxation (Cabedo et al., 2006a).

Storage modulus (E') of all CPN is higher than that of the pure EVOH throughout the full temperature range studied (Figure 6a). At temperatures below the α -relaxation, Kaol platelets have a *reinforcing* effect, increasing the value of the storage modulus (E') and decreasing the loss modulus (E''). This effect increases proportionally with the Kaol content of the sample. The difference in the DMA behaviour between the EVOH and the CPN is more evident at temperatures above T_g , however the dependence with the Kaol loading is not clear. Attending to the temperatures at which relaxations take place, the addition of the Kaol results in an increase in all three cases (α , α' , β). In the case of the α -relaxation, the maximum of the peak in the $\tan\delta$ curve of the CPN (see Figure 6b) is shifted over 15°C towards higher temperatures with respect to the pure EVOH. Loadings above 2.5% do not seem to enhance significantly this behaviour. From the DMA results, Kaol platelets seem to act as a reinforcing agent by increasing the elastic response of the matrix both at temperatures below and above the glass transition. The increase in the temperatures at which the relaxations take place could be explained by the fact that phyllosilicate platelets hinder chain mobility being thus necessary higher energies for relaxations to take place.

Table I gathers the results of the tensile tests conducted on films obtained from the co-extruded structures, both the pure EVOH and the CPN. The experiments were carried out in the machine direction (MD) as well as in the transversal direction (TD). Figure 7 plots the stress-strain curves of the samples analysed. According to the data, mechanical properties of EVOH copolymers are very dependent upon the direction of testing, hence

presenting more rigid and less ductile behaviour in MD than in TD. This behaviour can be attributed to the orientation of both the crystals and the polymer chains in the amorphous fraction in MD.

The addition of Kaol results in an increase of the elastic modulus (E), both in MD and TD, due to the reinforcing effect of clay mineral platelets. This effect is found to be more severe at higher Kaol loadings. Specifically, addition of 2.5% of Kaol increases the elastic modulus (E) value in 25% in MD and in 10% in TD; whereas a 5% Kaol loading results in an increase of the E of 80% in MD and 60% in TD. The increase in the elastic modulus is not correlated to an increase in the yield stress (σ_y), which remains almost unaffected in the EVOH/2.5Kaol sample, while is increased in MD in the EVOH/5Kaol sample. The considerable difference found between MD and TD when the clay was incorporated can be explained by a more severe orientation of the Kaol platelets and nanometric aggregates in the MD than in the TD. On the other hand, the addition of Kaol decreases the strain at break (ϵ_R).

3.3. Barrier properties of Kaolinite / EVOH nanocomposites.

Water weight loss permeation experiments for neat EVOH and the Kaol/EVOH nanocomposites are presented in Figure 8. The slope of the straight line is considerably lower in the case of the CPN than that of the pure copolymer. This fact reveals a clear enhancement on the water barrier with the addition of the Kaol. The calculated adsorption and diffusion coefficient of the three samples analysed are gathered in Table II. The addition of a 2.5% of Kaol to the pure matrix results in a decrease in water vapour permeability of 23%, whilst for the EVOH/5Kaol sample, the drop is above 46%. Together with the reduction in the water permeation rate, a decrease in the water diffusion coefficient has been found for the samples containing Kaol; specifically, this drop has been found to be of 20% in the case of the EVOH/2.5Kaol and of ca. 50% in the EVOH/5Kaol.

The oxygen barrier properties of the co-extruded samples were evaluated under dry conditions and under high relative humidity conditions (80%). Table III gathers the results obtained. The addition of Kaol to the EVOH matrix results in a considerable enhancement in the barrier properties to oxygen; e.g. under dry conditions, oxygen

permeability decreases 48% for the EVOH/2.5Kaol sample and up to 59% for the EVOH/5Kaol one. According to this, in high relative humidity conditions, the barrier to oxygen is improved by a 36% and 47% with a 2.5% and 5% Kaol loading respectively.

The improvement in the water and oxygen barrier properties it is due to an increase in the tortuosity of the diffusion path of the permeant throughout the polymeric film. This effect is more sever when all the clay mineral platelets and small sized aggregates are oriented perpendicularly to the diffusion direction, which is the case of the co-extruded films. The good interaction observed between the unmodified Kaol and the polymer matrix can also affect positively to this improvement.

4. Conclusions

From the results, it can be said that obtaining unmodified Kaol/EVOH nanocomposites by melt compounding is possible when the addition of the clay mineral is done by means of an appropriate Kaol/EVOH masterbatch; having these CPN enhanced properties for their application as high barrier material. From the morphological analysis it can be concluded that favourable morphology is achieved by blending in an internal mixer. However, full exfoliation has not been reached, as derived from the detection in all samples of nanometer-ranged aggregates. The presence of these structures is more common in the samples containing 7mass% Kaol loading.

DMA and tensile tests reveal a reinforcing effect of the Kaol platelets in the studied CPN, being higher their rigidity as well as the temperatures at which the matrix relaxations take place. Regarding the barrier properties, the presence of the nanofillers resulted in great enhancement to both water and oxygen. Hence, for the sample containing 5% of Kaol, the diffusion coefficient to water vapour was found to be reduced in 50%, while the oxygen permeability decreased up to 59% under dry conditions and 47% under high relative humidity conditions.

Acknowledgements

The authors would like to express their gratitude to Ms. Raquel Oliver and Mr. José Ortega for experimental support. The authors acknowledge Mr Y. Saito, The Nippon Synthetic Chemical Industry Co. Ltd (NIPPON GOHSEI), Japan, for supplying EVOH; Arciblansa S.A. for supplying the kaolinite.

References

- Alexandre, M., Dubois, P., 2000. Polymer-layered silicate nanocomposites: preparation, properties and uses of a new class of materials. *Mater. Sci. Eng. R Reports* 28, 1–63. doi:10.1016/S0927-796X(00)00012-7
- Arora, A., Padua, G.W., 2010. Review: nanocomposites in food packaging. *J. Food Sci.* 75, R43-9. doi:10.1111/j.1750-3841.2009.01456.x
- Bordes, P., Hablot, E., Pollet, E., Avérous, L., 2009. Effect of clay organomodifiers on degradation of polyhydroxyalkanoates. *Polym. Degrad. Stab.* 94, 789–796. doi:10.1016/j.polymdegradstab.2009.01.027
- Cabedo, L., 2007. Desarrollo de nanocompuestos basados en copolímeros de etileno y alcohol vinílico (EVOH) y filosilicatos laminares para su aplicación en envases de alta barrera. PhD Thesis. Universitat Jaume I.
- Cabedo, L., Giménez, E., Lagaron, J.M., Gavara, R., Saura, J.J., 2004. Development of EVOH-kaolinite nanocomposites. *Polymer (Guildf)*. 45, 5233–5238. doi:10.1016/j.polymer.2004.05.018
- Cabedo, L., Lagarón, J.M., Cava, D., Saura, J.J., Giménez, E., 2006a. The effect of ethylene content on the interaction between ethylene-vinyl alcohol copolymers and water—II: Influence of water sorption on the mechanical properties of EVOH copolymers. *Polym. Test.* 25, 860–867. doi:10.1016/j.polymertesting.2006.04.012
- Cabedo, L., Luis Feijoo, J., Pilar Villanueva, M., Lagarón, J.M., Giménez, E., 2006b. Optimization of Biodegradable Nanocomposites Based on aPLA/PCL Blends for Food Packaging Applications. *Macromol. Symp.* 233, 191–197. doi:10.1002/masy.200690017
- Cabedo, L., Plackett, D., Gimenez, E., Lagaron, J.M., 2009. Studying the Degradation of Polyhydroxybutyrate-co-valerate during Processing with Clay-Based Nanofillers. *J. Appl. Polym. Sci.* 112, 3669–3676. doi:10.1002/app.29945
- Cava, D., Cabedo, L., Gimenez, E., Gavara, R., Lagaron, J.M., 2006. The effect of ethylene content on the interaction between ethylene–vinyl alcohol copolymers and

water: (I) Application of FT-IR spectroscopy to determine transport properties and interactions in food packaging films. *Polym. Test.* 25, 254–261.
doi:10.1016/j.polymertesting.2005.09.018

Cerrada, M.L., Pérez, E., Pereña, J.M., Benavente, R., 1998. Wide-angle X-ray diffraction study of the phase behavior of vinyl alcohol-ethylene copolymers. *Macromolecules* 31, 2559–2564.

Chen, B., Evans, J.R.G., 2005. Thermoplastic starch – clay nanocomposites and their characteristics. *Carbohydr. Polym.* 61, 455–463.
doi:10.1016/j.carbpol.2005.06.020

Detellier and Letaief, 2013, Kaolinite Polymer Nanocomposites (Chapter 13.2) in *Handbook of Clay Science* (Bergaya and Lagaly, Eds.) Vol5A Developments of Clay Science, Elsevier

Fornes, T.D., Yoon, P.J., Paul, D.R., 2003. Polymer matrix degradation and color formation in melt processed nylon 6 / clay nanocomposites. *Polymer (Guildf)*. 44, 7545–7556. doi:10.1016/j.polymer.2003.09.034

Fukushima, K., Giménez, E., Cabedo, L., Lagarón, J.M., Feijoo, J.L., 2012. Biotic degradation of poly(dl-lactide) based nanocomposites. *Polym. Degrad. Stab.* 97, 1278–1284. doi:10.1016/j.polymdegradstab.2012.05.029

Gardolinski, J.E., Carrera, L.C.M., Cantão, M.P., Wypych, F., 2000. Layered polymer-kaolinite nanocomposites. *J. Mater. Sci.* 35, 3113–3119.
doi:10.1023/A:1004820003253

Giannelis, E.P., 1996. Polymer layered silicate nanocomposites. *Adv. Mater.* 8, 29–35.

Gimenez, E., Cabedo, L., Lagaron, J.M., Gavara, R., Saura, J.J., 2004. Development of EVOH-kaolinite nanocomposites for high barrier packaging applications, in: *Annual Technical Conference - ANTEC, Conference Proceedings*. pp. 2035–2039.

Kenne, G., Detellier, C., 2016. Applied Clay Science Functional nanohybrid materials derived from kaolinite. *Appl. Clay Sci.* In press. doi:10.1016/j.clay.2016.01.010

Kim, D., Kwon, H., Seo, J., 2014. EVOH nanocomposite films with enhanced barrier properties under high humidity conditions. *Polym. Compos.* 35, 644–654.
doi:10.1002/pc.22707

Kim, S.W., Cha, S.-H., 2014. Thermal, mechanical, and gas barrier properties of ethylene-vinyl alcohol copolymer-based nanocomposites for food packaging films: Effects of nanoclay loading. *J. Appl. Polym. Sci.* 131, n/a-n/a.
doi:10.1002/app.40289

- 432 Kotsilkova, R., Petkova, V., Pelovski, Y., 2001. Thermal analysis of polymer-silicate
433 nanocomposites. *J. Therm. Anal. ...* 64, 591–598.
- 434 Lagarón, J., Giménez, E., Gavara, R., Saura, J., Gime, E., 2001. Study of the influence
435 of water sorption in pure components and binary blends of high barrier ethylene–
436 vinyl alcohol copolymer and amorphous polyamide and nylon-containing ionomer.
437 *Polymer (Guildf)*. 42, 9531–9540. doi:10.1016/S0032-3861(01)00496-7
- 438 Lagarón, J.M., Cabedo, L., Cava, D., Feijoo, J.L., Gavara, R., Gimenez, E., 2005.
439 Improving packaged food quality and safety. Part 2: nanocomposites. *Food Addit.*
440 *Contam.* 22, 994–998. doi:10.1080/02652030500239656
- 441 Lagarón, J.M., Giménez, E., Saura, J.J., Gavara, R., 2001. Phase morphology,
442 crystallinity and mechanical properties of binary blends of high barrier ethylene–
443 vinyl alcohol copolymer and amorphous polyamide and a polyamide-containing
444 ionomer. *Polymer (Guildf)*. 42, 7381–7394. doi:10.1016/S0032-3861(01)00204-X
- 445 Lagaron, J.M., Powell, A.K., Bonner, G., 2001. Permeation of water, methanol, fuel and
446 alcohol-containing fuels in high-barrier ethylene–vinyl alcohol copolymer. *Polym.*
447 *Test.* 20, 569–577. doi:10.1016/S0142-9418(00)00077-5
- 448 Lambert and Bergaya, 2013, Smectite Polymer Nanocomposites (Chapter 13.1) in
449 *Handbook of Clay Science (Bergaya and Lagaly, Eds.) Vol5A Developments of*
450 *Clay Science*, Elsevier
- 451 Martínez-Sanz, M., Lopez-Rubio, A., Lagaron, J.M., 2012. Nanocomposites of ethylene
452 vinyl alcohol copolymer with thermally resistant cellulose nanowhiskers by melt
453 compounding (II): Water barrier and mechanical properties. *J. Appl. Polym. Sci.*
454 128, n/a-n/a. doi:10.1002/app.38432
- 455 Muramatsu, M., Okura, M., Kuboyama, K., Ougizawa, T., Yamamoto, T., Nishihara,
456 Y., Saito, Y., Ito, K., Hirata, K., Kobayashi, Y., 2003. Oxygen permeability and
457 free volume hole size in ethylene–vinyl alcohol copolymer film: temperature and
458 humidity dependence. *Radiat. Phys. Chem.* 68, 561–564. doi:10.1016/S0969-
459 806X(03)00231-7
- 460 Ophir, A., Dotan, A., Belinsky, I., Kenig, S., 2010. Barrier and mechanical properties of
461 nanocomposites based on polymer blends and organoclays. *J. Appl. Polym. Sci.*
462 116, 72–83. doi:10.1002/app.31285
- 463 Pavlidou, S., Papaspyrides, C.D., 2008. A review on polymer–layered silicate
464 nanocomposites. *Prog. Polym. Sci.* 33, 1119–1198.
465 doi:10.1016/j.progpolymsci.2008.07.008

- Schoonheydt, R.A., Johnston, C.T., Chapter 3 Surface and Interface Chemistry of Clay Minerals, In: Faïza Bergaya, Benny K.G. Theng and Gerhard Lagaly, Editor(s), Developments in Clay Science, Elsevier, 2006, Volume 1, Pages 87-113, [http://dx.doi.org/10.1016/S1572-4352\(05\)01003-2](http://dx.doi.org/10.1016/S1572-4352(05)01003-2).
- Sinha Ray, S., Okamoto, M., 2003. Polymer/layered silicate nanocomposites: a review from preparation to processing. *Prog. Polym. Sci.* 28, 1539–1641.
- Vahabi, H., Batistella, M.A., Otazaghine, B., Longuet, C., Ferry, L., Sonnier, R., Lopez-Cuesta, J.M., 2012. Influence of a treated kaolinite on the thermal degradation and flame retardancy of poly(methyl methacrylate). *Appl. Clay Sci.* 70, 58–66. doi:10.1016/j.clay.2012.09.013
- Villalpando-Olmos, J., Sánchez-Valdes, S., Yáñez-Flores, I.G., 1999. Performance of polyethylene/ethylene-vinyl alcohol copolymer/polyethylene multilayer films using maleated polyethylene blends. *Polym. Eng. Sci.* 39, 1597–1603.
- Villanueva, M.P., Cabedo, L., Lagaron, J.M., Giménez, E., 2010. Comparative study of nanocomposites of polyolefin compatibilizers containing kaolinite and montmorillonite organoclays. *J. Appl. Polym. Sci.* 115, 1325–1335. doi:10.1002/app.30278
- Wan, C., Qiao, X., Zhang, Y., Zhang, Y., 2003. Effect of different clay treatment on morphology and mechanical properties of PVC-clay nanocomposites. *Polym. Test.* 22, 453–461. doi:10.1016/S0142-9418(02)00126-5
- Xia, Y., Rubino, M., Auras, R., 2015. Release of surfactants from organo-modified montmorillonite into solvents: Implications for polymer nanocomposites. *Appl. Clay Sci.* 105–106, 107–112. doi:10.1016/j.clay.2014.12.027
- Yoshihiko, K., Yoshiyuki, S., Kuroda, K., 1999. Intercalation of alkylamines and water into kaolinite with methanol kaolinite as an intermediate. *Appl. Clay Sci.* 15, 241–252. doi:10.1016/S0169-1317(99)00014-9
- Zhang, Y., Liu, Q., Zhang, S., Zhang, Y., Zhang, Y., Liang, P., 2016. Characterization of kaolinite/styrene butadiene rubber composite: Mechanical properties and thermal stability. *Appl. Clay Sci.* 124–125, 167–174. doi:<http://dx.doi.org/10.1016/j.clay.2016.02.002>
- Zulfiqar, S., Sarwar, M.I., Rasheed, N., Yavuz, C.T., 2015. Influence of interlayer functionalization of kaolinite on property profile of copolymer nanocomposites. *Appl. Clay Sci.* 112–113, 25–31. doi:10.1016/j.clay.2015.04.010

	500	[
1		
2	501	
3		
4	502	
5		
6		
7		
8		
9		
10		
11		
12		
13		
14		
15		
16		
17		
18		
19		
20		
21		
22		
23		
24		
25		
26		
27		
28		
29		
30		
31		
32		
33		
34		
35		
36		
37		
38		
39		
40		
41		
42		
43		
44		
45		
46		
47		
48		
49		
50		
51		
52		
53		
54		
55		
56		
57		
58		
59		
60		
61		
62		
63		
64		
65		

Figure Captions:

Figure 1: SEM micrograph (a) and WAXS pattern (b) of the Kaol.

Figure 2: WAXS patterns of the masterbatch and the Kaol/EVOH nanocomposites.

Figure 3: SEM micrographs of masterbatch powder. The white arrows indicate the presence of small clay aggregates.

Figure 4: SEM micrographs of crio fractured surface of the EVOH/5Kaol (a) and EVOH/7Kaol (b) samples. The white arrows indicate the presence of small clay aggregates.

Figure 5: TEM micrographs of Kaol/EVOH nanocomposites: a) EVOH/5Kaol and b) EVOH/7Kaol.

Figure 6: DMA curves of the pure EVOH and the Kaol/EVOH nanocomposites: a) Storage modulus (E') and loss modulus (E'') vs. temperature, b) $\tan\delta$ vs. temperature.

Figure 7: Stress-strain curves of the co-extruded EVOH and Kaol/EVOH nanocomposites in machine direction (MD) and in the transverse direction (TD).

Figure 8: Direct permeability to water vapour of pure co-extruded EVOH and co-extruded EVOH CPN.

522 **Table Headings:**
523
524 **Table I:** Tensile tests results of the pure EVOH and the Kaol/EVOH nanocomposites
525 obtained by co-extrusion.
526 **Table II:** Permeability (P), solubility (S) and diffusion (D) to water vapour of the co-
527 extruded samples.
528 **Table III:** Oxygen permeability and reduction with respect to the EVOH of the co-
529 extruded samples under dry conditions and at 80% R.H.
530
531
532

- Nanocomposites of unmodified kaolinite / EVOH have been obtained by melt blending
- Kaolinite/EVOH nanocomposites exhibited improved mechanical and thermal performance
- The water diffusion coefficient in the nanocomposites decreased by 50%
- Oxygen barrier of the nanocomposites (dry and high humidity) was increased by 50%

1 **Table I:** Cabedo et al.

Direction	Sample	E (GPa)	σ_y (MPa)	σ_R (MPa)	ϵ_R (%)
MD	EVOH	2.4±0.2	78±4	66±5	13±1
	EVOH/2.5Kao	3.0±0.2	78±4	70±4	12±4
	EVOH/5Kao	4.3±0.4	95±8	86±8	10±1
TD	EVOH	2.2±0.2	75±1	59±3	35±4
	EVOH/2.5Kao	2.4±0.5	68±4	58±3	15±2
	EVOH/5Kao	3.5±0.3	75±4	62±1	23±10

2
3
4

1 **Table II:** Cabedo et al.

2

	P (kg·m/s·m²·Pa)	S (kg/m³Pa)	D(m²/s)
<i>EVOH</i>	1.94·10 ⁻¹⁶	0.048	4.04·10 ⁻¹⁵
<i>EVOH/2.5Kao</i>	1.49·10 ⁻¹⁶	0.046	3.24·10 ⁻¹⁵
<i>EVOH/5Kao</i>	1.05·10 ⁻¹⁶	0.051	2.06·10 ⁻¹⁵

3

4

5

1 **Table III:** Cabedo et al.

2

	$P_{O_2} (m^3 m/m^2 sPa)$			
	24°C y 0%R.H.		24°C y 80%R.H.	
<i>EVOH</i>	$2.9 \cdot 10^{-21}$	----	$4.5 \cdot 10^{-21}$	----
<i>EVOH/2.5Kao</i>	$1.5 \cdot 10^{-21}$	48%	$2.9 \cdot 10^{-21}$	36%
<i>EVOH/5Kao</i>	$1.2 \cdot 10^{-21}$	59%	$2.4 \cdot 10^{-21}$	47%

3

Figure 1
[Click here to download high resolution image](#)

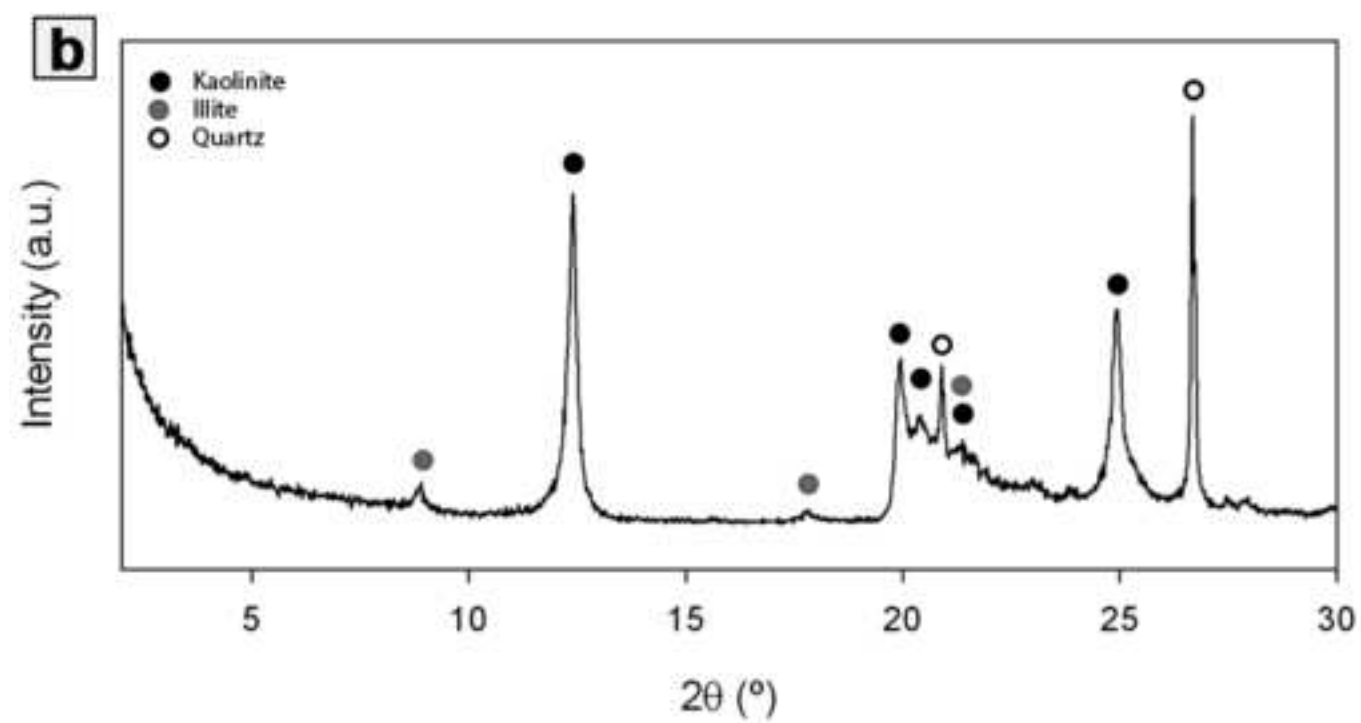
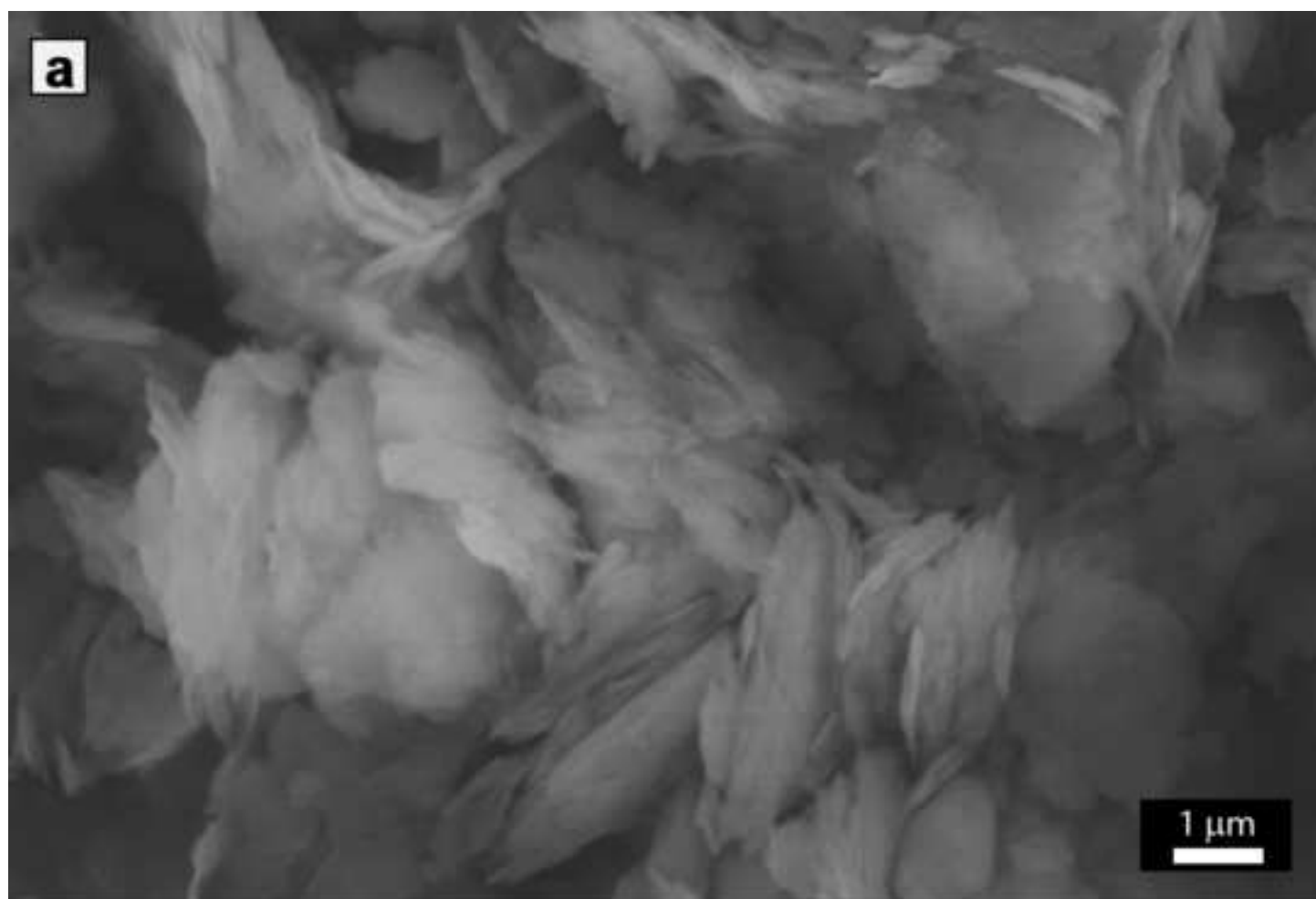


Figure 2
[Click here to download high resolution image](#)

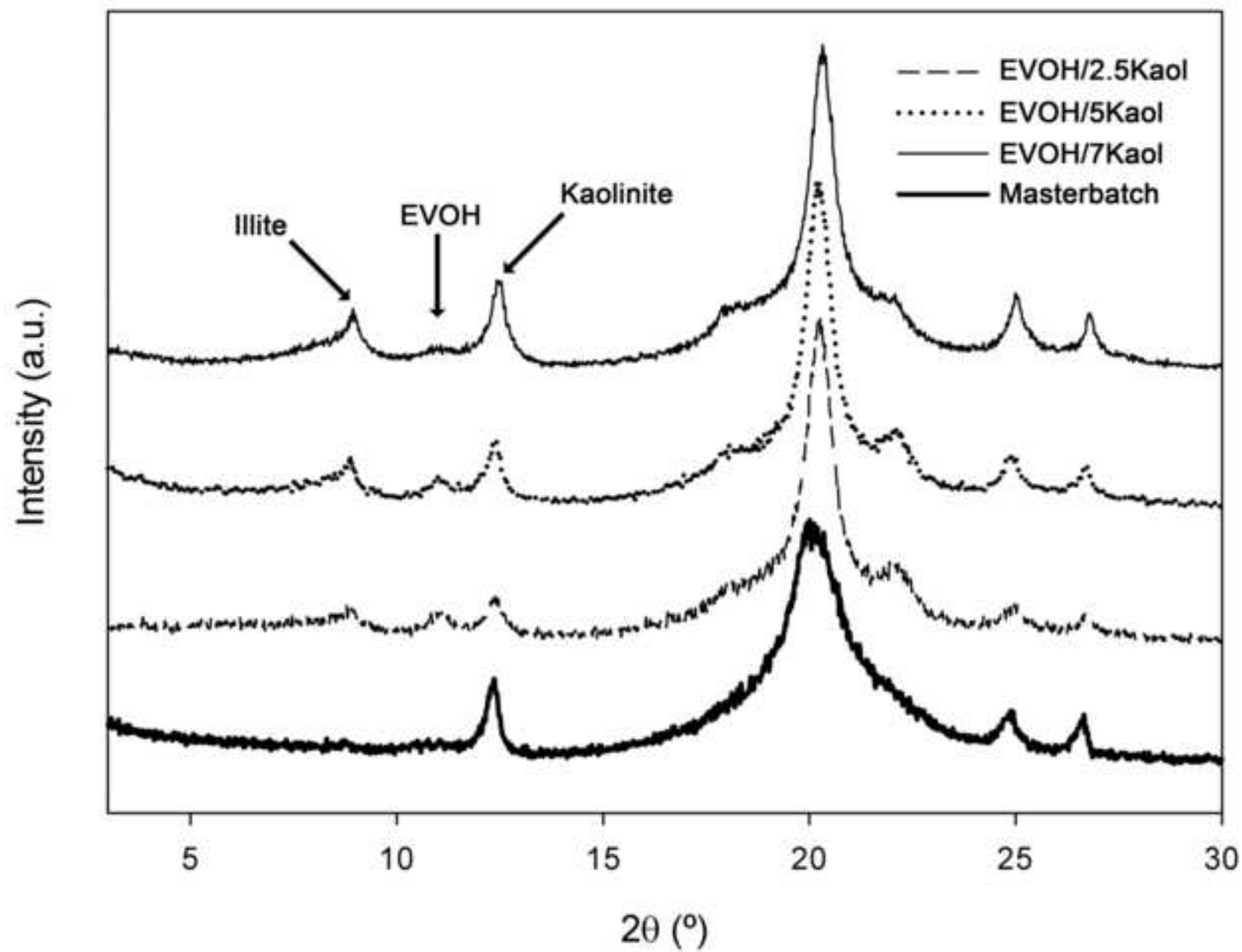


Figure 3
[Click here to download high resolution image](#)

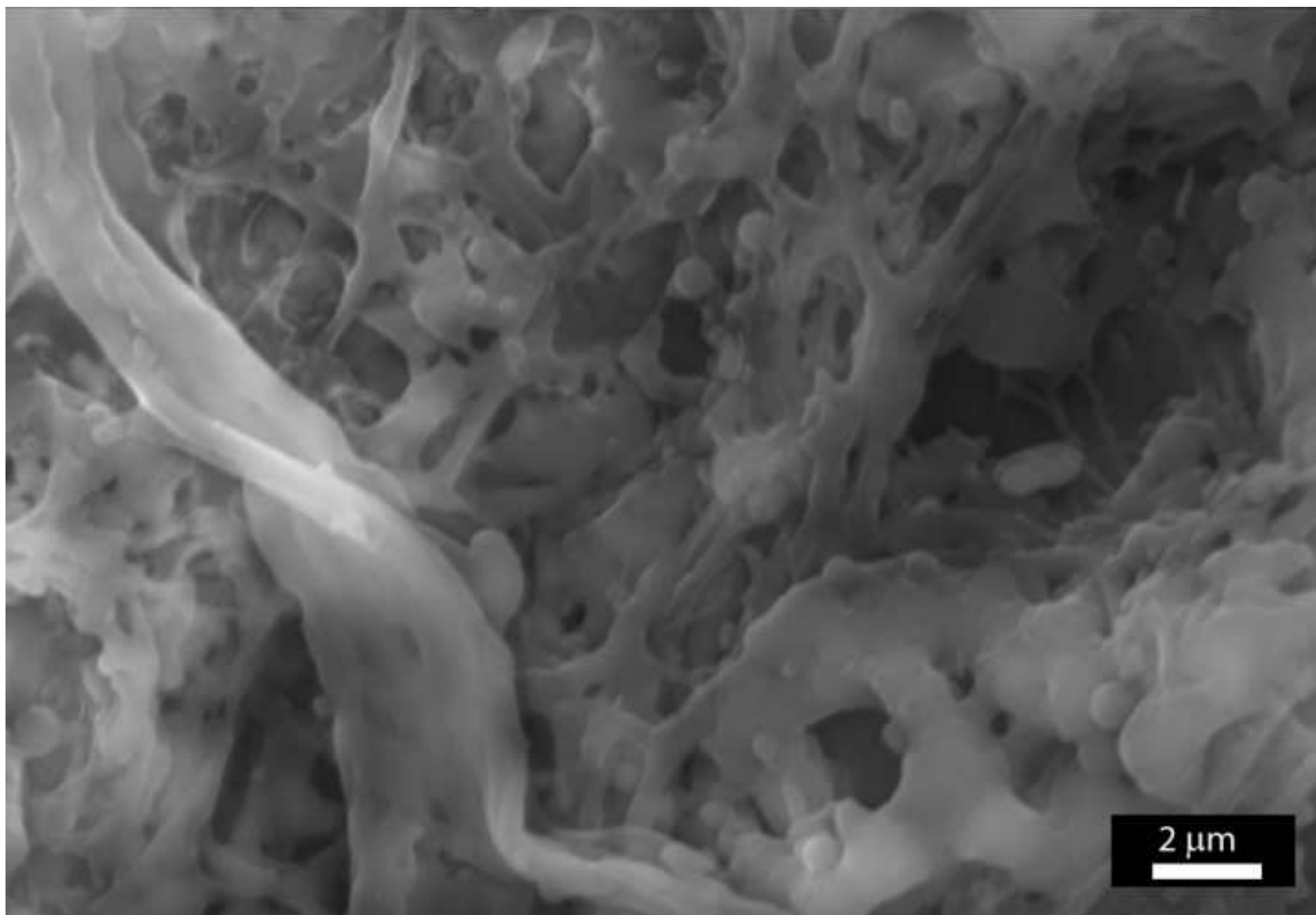


Figure 4
[Click here to download high resolution image](#)

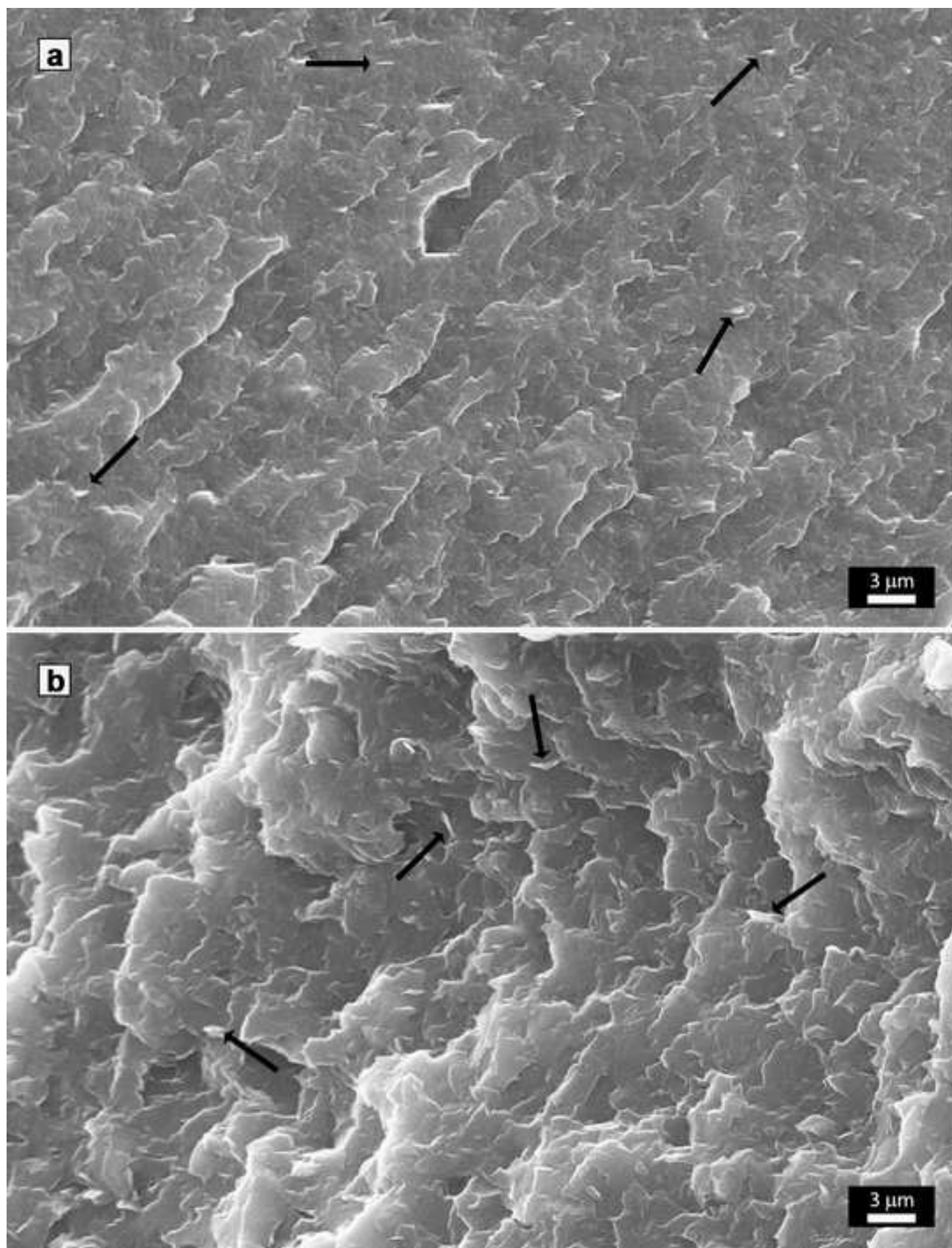


Figure 5
[Click here to download high resolution image](#)

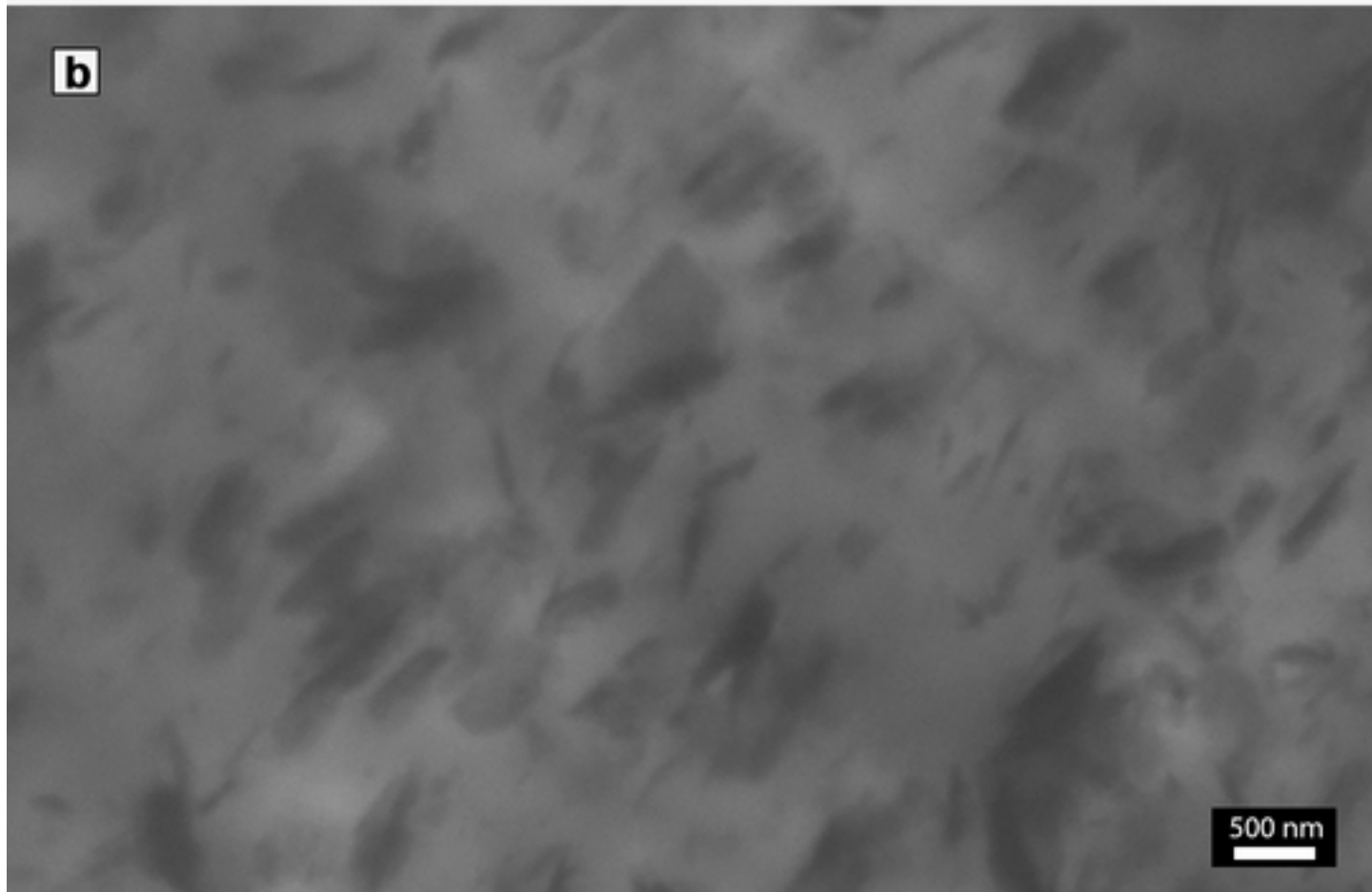


Figure 6
[Click here to download high resolution image](#)

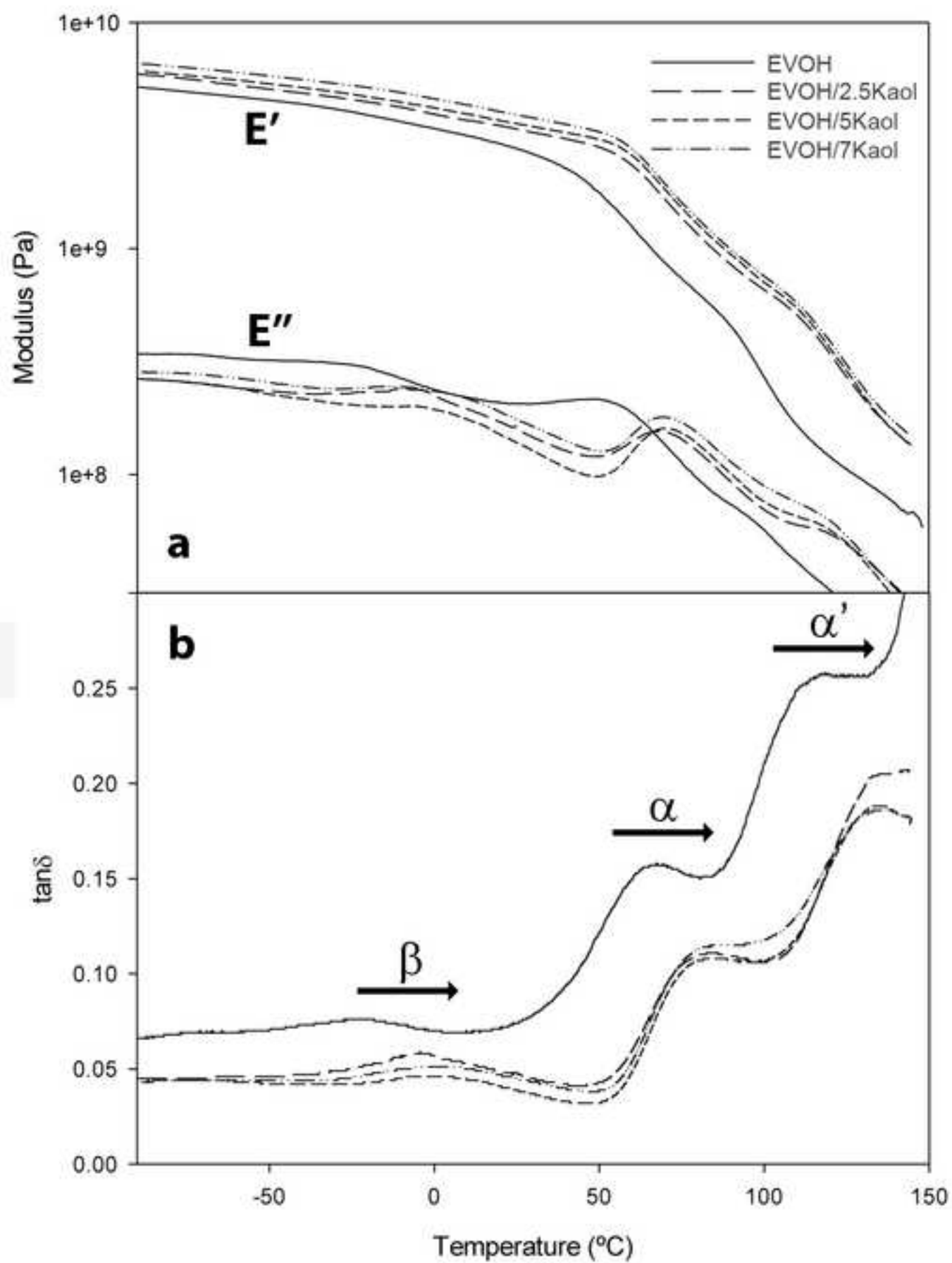


Figure 7
[Click here to download high resolution image](#)

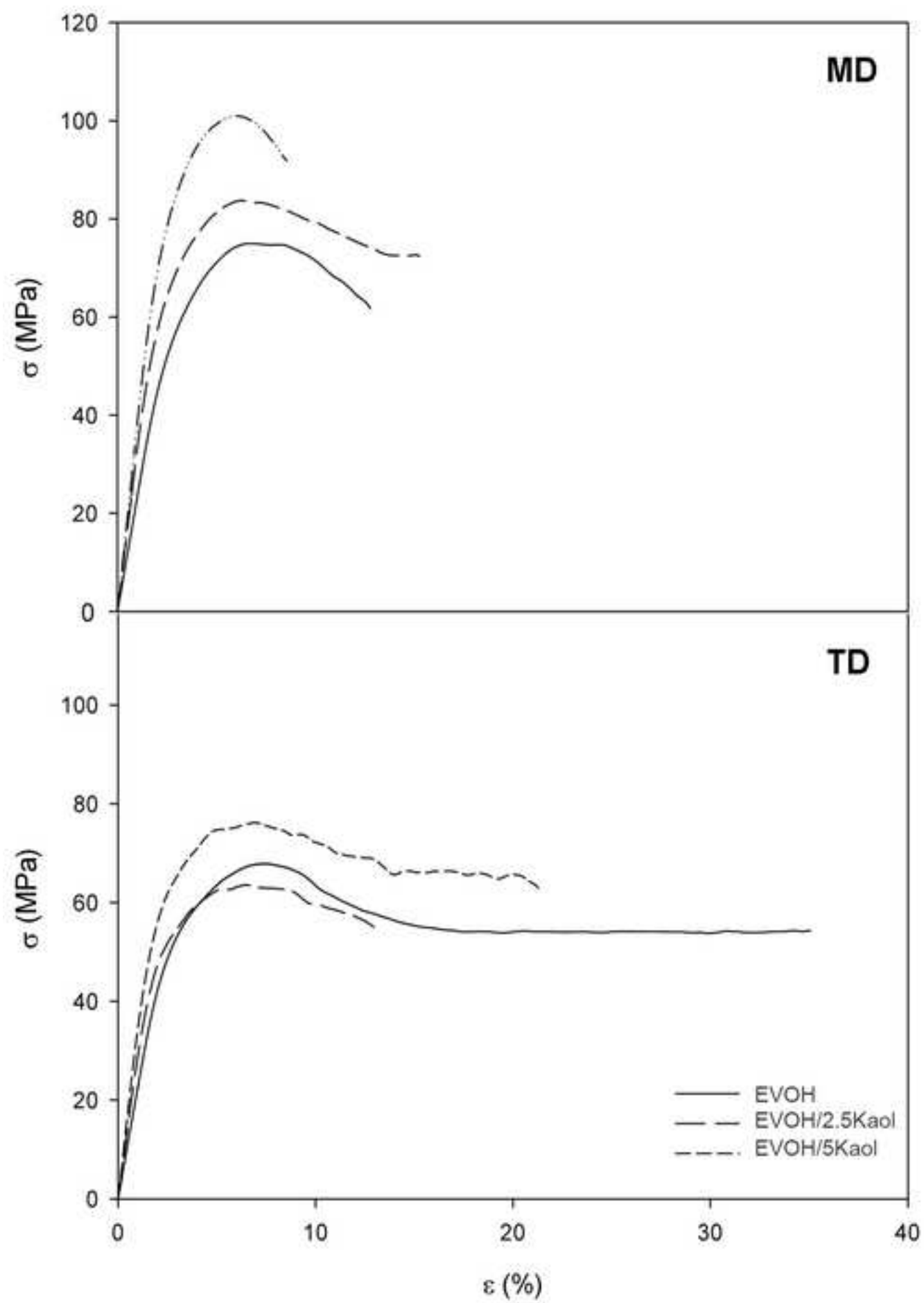
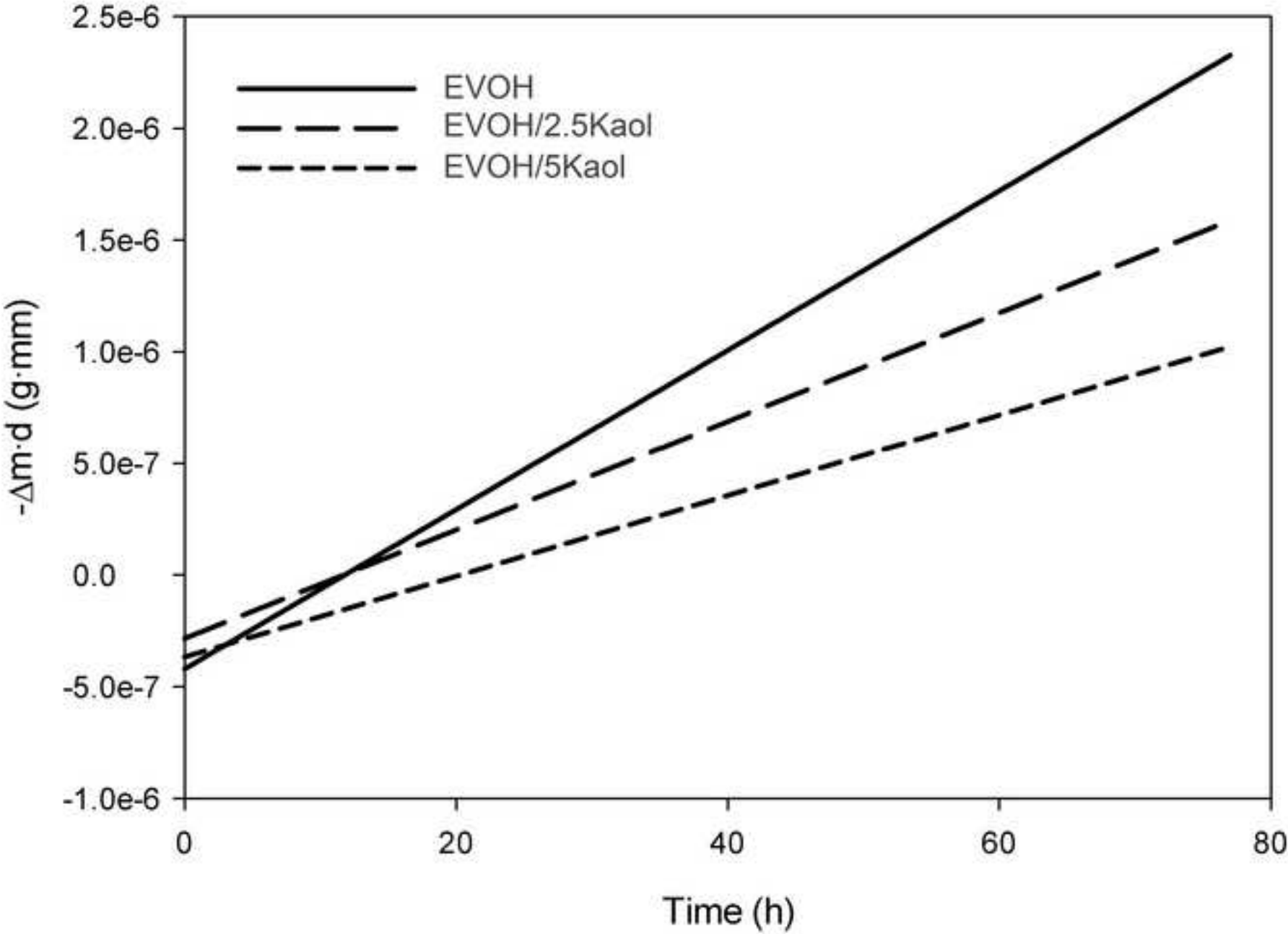


Figure 8
[Click here to download high resolution image](#)



Abstract

Nanocomposites of unmodified kaolinite (Kaol) / ethylene-vinyl alcohol copolymer (EVOH) with different Kaol contents have been obtained by a two-step process: melt blending in an internal mixer and film processing by co-extruding the obtained clay polymer nanocomposites pellets in between two low-density polyethylene (LDPE) layers. The addition of the clay mineral to the molten polymer has been carried out by using a Kaol/EVOH masterbatch containing 15mass% Kaol. The so-obtained samples have been analysed by means of WAXS, SEM, TEM, DMA and tensile tests. Finally, barrier properties to water vapour and oxygen at two relative humidities have been assessed. Morphological analysis has revealed high degree of dispersion and distribution of the Kaol within the EVOH matrix. A considerable increase in the mechanical and in the barrier properties has been found. The present work puts forward the effectiveness of an unmodified kaolinite for obtaining ultra-high barrier clay mineral / polymer nanocomposites.